Journal of Safety Research 49 (2014) 1

Contents lists available at ScienceDirect

Journal of Safety Research

journal homepage: www.elsevier.com/locate/jsr

Editorial

Letter from the Editors

The *Journal of Safety Research* is pleased to publish in this special issue the proceedings of several papers presented at the 4th International Conference on Road Safety and Simulation convened at Roma Tre University in Rome, Italy, October 2013. This conference serves as an interdisciplinary forum for the exchange of ideas, methodologies, research, and applications aimed at improving road safety globally.

Conference proceedings provide the opportunity for research in its formative stages to be shared, allowing our readers to gain early insights in the type of work currently being conducted and for the researchers to receive valuable feedback to help inform ongoing activities. This conference in particular offers an array of research topics not often covered by this journal from researchers practicing in over 11 countries. As is common with publishing conference proceedings, the papers published in this issue did not go through the normal *JSR* review process. Each paper included in this issue did meet the Road Safety and Simulation conference review requirements. They reflect varying degrees of scientific rigor, methodological design, and groundbreaking application.

The proceedings published in this special issue of *JSR* draw from the following road safety research sectors represented at the conference: driving simulation, crash causality, naturalistic driving, and new research methods.

It is our hope that the publication of these important proceedings will stimulate vigorous dialogue, rigorous research, and continuing innovative initiatives and applications, leading, ultimately, to fewer traffic fatalities, injuries, and crashes.

Thomas W. Planek
Editor-in-Chief

Sergey Sinelnikov
Associate Editor

Jonathan Thomas
Associate Editor

Kenneth Kolosh
Associate Editor

Kathleen Porretta
Managing Editor

18 February 2014

http://dx.doi.org/10.1016/j.jsr.2014.02.001

Journal of Safety Research 49 (2014) 105–112

Contents lists available at ScienceDirect

Journal of Safety Research

journal homepage: www.elsevier.com/locate/jsr

On the required complexity of vehicle dynamic models for use in simulation-based highway design

Alexander Brown [a], Sean Brennan [b,*]

[a] Penn State University, 201 Transportation Research Building, University Park, PA 16802, USA
[b] Mechanical Engineering, Penn State University, 157D Hammond Building, University Park, PA 16802, USA

ARTICLE INFO

Article history:
Received 21 October 2013
Accepted 4 March 2014
Available online 24 April 2014

Keywords:
Friction
Modeling
Simulation
Highway safety
Vehicle dynamics

ABSTRACT

Introduction: This paper presents the results of a comprehensive project whose goal is to identify roadway design practices that maximize the margin of safety between the friction supply and friction demand. This study is motivated by the concern for increased accident rates on curves with steep downgrades, geometries that contain features that interact in all three dimensions — planar curves, grade, and superelevation. This complexity makes the prediction of vehicle skidding quite difficult, particularly for simple simulation models that have historically been used for road geometry design guidance. *Method:* To obtain estimates of friction margin, this study considers a range of vehicle models, including: a point-mass model used by the American Association of State Highway Transportation Officials (AASHTO) design policy, a steady-state "bicycle model" formulation that considers only per-axle forces, a transient formulation of the bicycle model commonly used in vehicle stability control systems, and finally, a full multi-body simulation (CarSim and TruckSim) regularly used in the automotive industry for high-fidelity vehicle behavior prediction. The presence of skidding – the friction demand exceeding supply – was calculated for each model considering a wide range of vehicles and road situations. *Results:* The results indicate that the most complicated vehicle models are generally unnecessary for predicting skidding events. However, there are specific maneuvers, namely braking events within lane changes and curves, which consistently predict the worst-case friction margins across all models. This suggests that any vehicle model used for roadway safety analysis should include the effects of combined cornering and braking. *Practical Implications:* The point-mass model typically used by highway design professionals may not be appropriate to predict vehicle behavior on high-speed curves during braking in low-friction situations. However, engineers can use the results of this study to help select the appropriate vehicle dynamic model complexity to use in the highway design process.

1. Introduction

This paper presents the results of a comprehensive three-year project to predict vehicle skidding events on roads of differing geometry. The goal of these simulations is to identify roadway design practices that maximize the margin of safety between the friction demanded by users of the roadway and the maximum friction that can be supplied on the roadway during normal operation. This study is motivated by the concern for increased accident rates in areas that have steep downgrades combined with sharp curves. Such downgrades often occur in mountainous areas, and the difficult terrain of these areas often requires the use of minimum-radius curves as per current highway design rules. Design practice for minimum-radius curves is to use "superelevation," or banked curves, to enable tighter turn geometries while presumably maintaining reasonable lateral friction demand from the vehicle's tires. Thus, steep downgrade curves contain features that interact in all three dimensions — planar curves, grade, and superelevation. This complexity makes the prediction of vehicle skidding quite difficult, particularly for simple simulation models that have historically been used for road geometry design guidance, a fact that has motivated research into road measurement for vehicle simulation purposes (Chemistruck, Detweiler, Ferris, Reid, & Gorsich, 2009; Dembski, Rizzoni, Soliman, Malmedahl, & Disaro, 2006; Detweiler & Ferris, 2010; Kern & Ferris, 2007; Stine, Hamblin, Brennan, & Donnell, 2010).

A specific challenge in this study is therefore to identify models of suitable complexity to accurately predict friction demand on a 3D roadway, but at the same time be simple enough to facilitate broad, sweeping studies of roadway design variations. These models must be based on physically measurable properties – road friction values, vehicle geometries, vehicle inertial properties, road geometries, and so forth – and must be verifiable via field measurements. The range of

* Corresponding author.
E-mail addresses: aab5009@psu.edu (A. Brown), sbrennan@psu.edu (S. Brennan).

http://dx.doi.org/10.1016/j.jsr.2014.03.005
0022-4375/

models included in this study is obtained from roadway design guidance and vehicle chassis control practice, and includes a point-mass model used by the American Association of Highway Transportation Officials (AASHTO) in present design policy (AASHTO, 2011), a steady-state "bicycle model" formulation that considers only per-axle forces (Pacejka, 2006), a transient formulation of the bicycle model commonly used in vehicle stability control systems (Pacejka, 2006), and finally a full multi-body simulation (CarSim and TruckSim) regularly used in the automotive industry for high-fidelity vehicle behavior prediction. The overall goal of the simulation effort is to examine whether operating conditions commonplace in standard driving practices require modifications to existing AASHTO design policy based on the results of simulation of each of the vehicle models.

2. Simulation Approach

A challenge in the use of any simulation is that errors in the assumptions or setup will produce errors in the simulation output. Generally, a higher fidelity simulation will produce more accurate predictions, but with very severe computational burdens and often with exponentially more simulation parameters to study. For example, the so-called "point-mass model" depends on very few parameters and can be simulated across all vehicles and road situations in the feasible design space in less than a second using a modestly powered computer. In contrast, a multi-body simulation (e.g., CarSim) depends on hundreds to thousands of vehicle parameters, and may take tens of seconds to simulate and post-process data across just one road profile, for one vehicle. One expects a multi-body simulation to be more accurate, particularly since these are in heavy use by industry, but it quickly becomes impractical to use complex software to analyze primary design decisions for road geometry. Further, one expects that at some point, adding additional simulation detail does not perceptibly affect the results. Thus, it is possible to "over-complicate" a simulation with corresponding computational penalties and obfuscation of primary results.

One way to balance a simulation approach between over-simplification versus over-complication is to compare simulations of increasing fidelity to one another across common road use scenarios. It can be expected that the simplest models will produce substantial error in their outputs, which are discoverable by noting large differences in predictions using these simple models to simulations of greater fidelity. Similarly, simulation models that are too complex will have predictions that are little changed from simpler models.

The simulation approach of this study used models of increasing complexity to determine a vehicle's friction demand. For each simulation, the primary focus was to determine whether friction demand, f, exceeds the supply friction, $f_{tire-pavement}$, margin, consider the simple definition in Eq. (1):

$$f_{margin} = f_{y,supply} - f_y. \tag{1}$$

In other words, the lateral friction margin is defined as lateral friction supply minus the lateral friction (i.e., cornering friction).

Situations of zero or negative friction margins must be avoided because a vehicle will skid and be unable to maintain the desired trajectory along the horizontal alignment of the road. For each analysis, the $f_{tire-pavement}$ values are represented by a friction ellipse that encompasses the maximum friction supply in the longitudinal or x-direction (braking) and lateral or y-direction (side) as shown in Fig. 1. The operating situation of the vehicle including the driver's inputs, vehicle type, vehicle loading, and so forth will determine the tire forces and hence the "friction demand" imposed by the vehicle; usually, this operating point will be within the friction ellipse. The outer boundary of the road's tire friction ellipse (e.g., the friction "supply") will change as a function of speed, tire type, and pavement condition; additional details on how the supply friction was obtained are in later sections. Because this study is focused on using vehicle models for roadway design, each

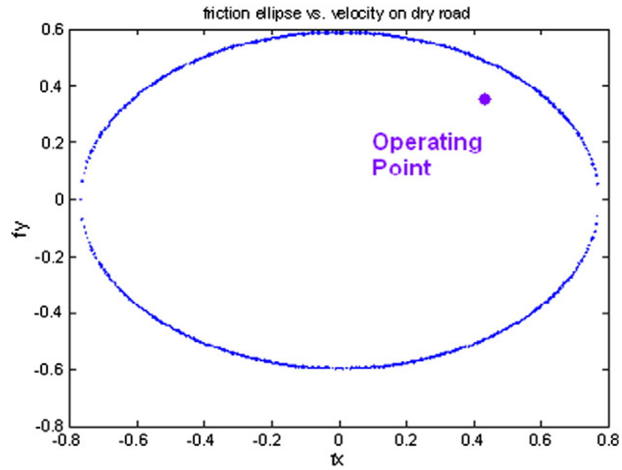

Fig. 1. Friction ellipse (tire–road model).

simulation is studied considering only changes in vehicle type, curve radius, the superelevation, steering maneuvers (curve-keeping versus lane-change), and braking type (no braking, curve-entry braking, stopping-sight braking, and emergency braking).

To define a suitable measure of friction margin for the simulations, the position of the operating point relative to the edge of the friction ellipse in Fig. 1 must be converted into a friction margin. One can see that using cornering friction (the vertical position in Fig. 1) alone does not quantify the proximity of the operating point to the edge of the friction ellipse, as braking maneuvers will move the operating point to the left and right. Instead, the *total friction* demand, not just the horizontal (i.e., cornering) friction, must be taken into account. The friction ellipse predicts that braking demands will decrease available lateral supply friction below the nominal value of $f_{y,max}$. The following modification is made to $f_{y,max}$ to obtain $f_{y,supply}$ by utilizing the friction ellipse equation:

$$f_{y,supply} = f_{y,max}\sqrt{1-\left(\frac{f_x}{f_{x,max}}\right)^2}. \tag{2}$$

This definition of lateral friction supply gives priority to braking margins first, which is consistent with how a vehicle operates in practice where a brake-induced skid event reduces lateral friction supply to near-zero values. Combining Eqs. (1) and (2), we obtain a usable definition of the lateral friction margin:

$$f_{margin} = f_{y,max}\sqrt{1-\left(\frac{f_x}{f_{x,max}}\right)^2} - f_y. \tag{3}$$

This definition of the lateral friction margin therefore depends on the tire's demanded side force, f_y, the demanded braking, f_x, and the maximum dimensions of the friction ellipse in the braking and lateral directions, $f_{x,max}$ and $f_{y,max}$. This friction margin definition is used in all simulations regardless of the complexity or structure of the simulation. For example, when using the modified point-mass model, the "tire" considered is actually a lumped representation of the sum of forces on *all tires* possessed by the real vehicle. When considering the per-axle (bicycle) model, each "tire" considered represents two tires lumped together, or even eight tires in the case of the rear tractor and trailer axles. For the per-tire simulations using high-order multi-body simulation software, the "tire" considered is consistent with a single "tire" on the physical vehicle. This is important because changing normal loads during a simulation due to weight transfer affects the ultimate supply friction available on true tires due to tire load sensitivity, and also changes the friction demand on each modeled tire as the model structure complexity increases to approach reality.

To summarize, the procedure for calculating lateral friction margin is consistent through all simulations and consists of the following steps:

1. Assuming wet road conditions (0.5 mm water depth), obtain a friction ellipse for the tire considered using a tire model, the tire type (passenger or truck tire), vehicle operating speed, and the friction data collected in the field.
2. Run a simulation of a vehicle traversing the hypothetical geometries under dry road conditions to obtain values for the demanded lateral and braking forces, F_x and F_y. Convert these to normalized forces, f_y and f_x (demanded friction) for any and all individual tires and/or tire groups present in the simulation.
3. Use the friction ellipse and f_x to obtain values of $f_{y,supply}$ for the simulated scenario per Eq. (2).
4. Calculate lateral friction margin as $f_{margin} = f_{y,supply} - f_y$ per Eq. (3).

For modern roadway designs in nominal conditions, the lateral friction margins are usually quite high. This is a result of the very conservative AASHTO policy for horizontal curve design, which is used for design of roadways. This study is constrained to curves with a minimum constant-radius design, so the radius, $R_{\min}$, is given by the AASHTO design rule:

$$R_{\min} = \frac{{V_{DS}}^2}{g \cdot (f_{\max} + 0.01 \cdot e_{\max})} \quad (4)$$

where V_{DS} is the roadway design speed, g is the gravitational constant, f_{max} is the maximum “design friction” assumed for the road (this is specified by the AASHTO policy as well), and e_{max} is the maximum superelevation of the road, generally less than 12% of bank angle. This equation illustrates that the present AASHTO roadway design policy does not utilize the friction ellipse concept, and thus driving maneuvers that require braking inputs can potentially generate negative friction margins.

3. Simulation Models

3.1. Point-Mass Model

For a given curve radius, superelevation, grade, and design speed, one can calculate the force balance on a point mass representation of a vehicle. To develop the point-mass model, the assumption of small angle representation (i.e. $cos\theta = 1$ and $sin\theta = \theta$) is made to maintain simplicity within equations; the angles of the road geometry are so small that these approximations are quite valid. The free body diagrams for the point mass model are shown in Fig. 2. Here, N represents the normal force from the road on the vehicle, F_b and F_c represent the braking and cornering forces acting on the vehicle point mass while γ and α represent the grade and superelevation angles, respectively. The deceleration, a_x, is directed along the vehicle's longitudinal axis. After applying a force balance using Newton's second law for a body rotating with angular velocity around a curve with constant radius, R, the three governing equations for vehicle motion in the X, Y, and Z-directions can be obtained (for more detail, see Varunjikar, 2011).

$$F_b = ma_x - mgsin\gamma = ma_x - mg\frac{G}{100} \quad (5)$$

$$F_c = m\frac{V^2}{R} - mgsin\alpha = m\frac{V^2}{R} - mg\frac{e}{100} \quad (6)$$

These equations can be simplified by substituting $N = mg$ and then simplifying the result using the friction definitions, $f_x = \frac{F_b}{N}$, and $f_y = \frac{F_c}{N}$:

$$f_x = \frac{a_x}{g} - \frac{G}{100} \quad (7)$$

$$f_y = \frac{V^2}{gR} - \frac{e}{100}. \quad (8)$$

Here, the terms f_x and f_y represent the friction demand in the braking (longitudinal) and cornering (lateral) directions. These depend on: a_x which is the braking-induced deceleration (which is positive for braking demands), g which is the gravitational constant, G which is the road grade (which is negative for downgrades), V which is the vehicle forward speed, R which is the curve radius, and e which is the road superelevation (positive values lean the vehicle to the inside of the curve). Comparing these equations to Eq. (4) used by AASHTO for minimum-radius curve design, we see that Eq. (8) is equivalent, while Eq. (7) adds an additional equation for the longitudinal friction factor. Thus, in the absence of braking forces, this point-mass vehicle will have the same lateral friction margins for each superelevation and grade due to the AASHTO design policy. With the addition of braking forces, however, the conditions change slightly as the total friction demand of a point-mass model for a vehicle is represented by f_x and f_y together. Note that this model has no provisions for analyzing transient maneuvers like lane changes. These maneuvers can only be captured by a more complex model of vehicle dynamics.

4. Steady-State Bicycle Model

A primary criticism of the point-mass model is that it does not account for the per-axle force generation capabilities of a vehicle. A typical passenger vehicle has an approximately 60/40 weight split from front to rear. When the vehicle is in a curve, this weight difference means that the lateral forces required on the front axle are usually much different than the rear axle. Indeed, the lateral forces required on each axle are proportional to the mass distributed over each axle; thus, on a flat road (i.e., one with no superelevation or grade), the weight distribution on the tires is exactly the same proportion as the lateral forces required from each axle. This is beneficial to curves on level roads: the vertical forces pushing down on each axle are pushing most on the axles that most need cornering forces. The net effect is that, for level roads, the weight differences are generally ignored for friction analysis without much error.

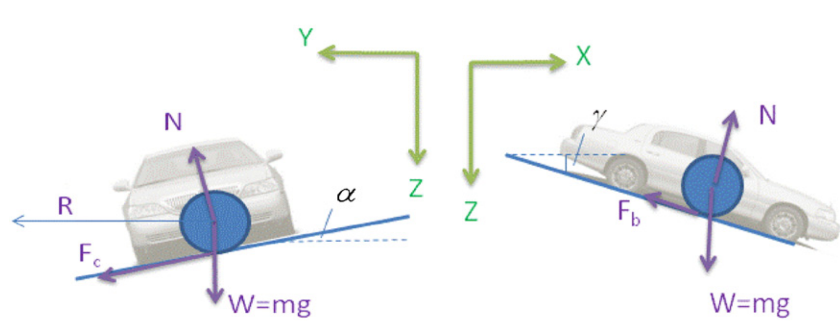

Fig. 2. Longitudinal forces acting on a vehicle point-mass model.

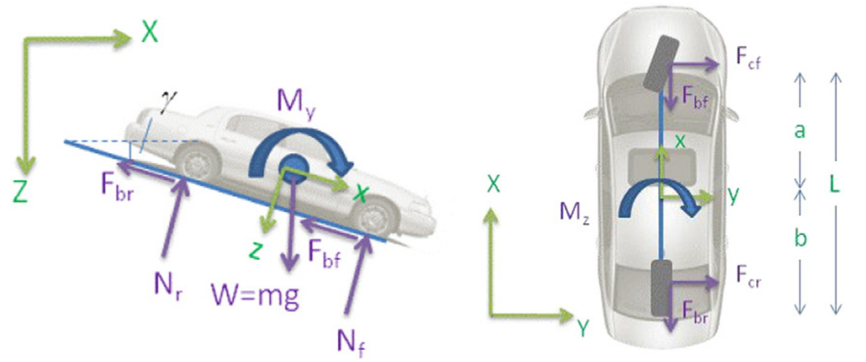

Fig. 3. Forces and moments acting on a vehicle in a steady turn on a superelevated curve with a downgrade.

However, on grades and in cases where there is deceleration, the weight shift from the rear to the front of the vehicle may significantly change the relative amounts of vertical tire force on each axle. If there is a curve on a grade, the cornering forces required from each axle remain proportional to the mass above each axle, not the weight. This difference between the mass-related cornering forces and the weight-related friction supply illustrates why curves on grades are so problematic for ensuring sufficient lateral friction margins.

To calculate this effect of per-axle friction utilization, this analysis uses a common simplification in vehicle dynamics: the vehicle is idealized as a rigid beam, and each axle is represented as a single tire situated at the midline of the vehicle. There are a number of additional assumptions in deriving this model, and details can be found in vehicle dynamics textbooks (e.g., Pacejka, 2006). The resulting model is termed a "bicycle model" because of its appearance (see Fig. 3).

The equations of motion for even the steady-state bicycle model are too involved for the brief presentation allowed in this paper, and the interested reader is referred to Pacejka (2006) for additional details. However, the general process is similar to that used for the point-mass model: the force balances in the lateral, longitudinal, and vertical directions are derived. For the bicycle model, the additional moment equations are also obtained in the vertical and lateral directions. The normal forces are solved for in terms of vehicle geometry, and are substituted into the cornering force equations. The resulting equations are then rearranged to solve for lateral friction factors for the front and rear axles. Noting that the weight of the vehicle, $W = mg$, the closed-form expressions for the side friction factors per axle are:

$$f_{yf} = \frac{F_{cf}}{N_f} = \frac{\frac{b}{L}\left(\frac{mV^2}{R} - W\frac{e}{100}\right)}{W\frac{b}{L} + \left(m\left(a_x - g\frac{G}{100}\right)\right)\frac{h}{L}}$$
$$f_{yf} = \frac{F_{cr}}{N_r} = \frac{\frac{b}{L}\left(\frac{mV^2}{R} - W\frac{e}{100}\right)}{W\frac{a}{L} - \left(m\left(a_x - g\frac{G}{100}\right)\right)\frac{h}{L}}. \quad (9)$$

These represent the quasi-static friction demands on the front and rear axles. Here G is the road grade, and e is the road superelevation as defined before. The terms a, b, L, and h are length parameters as shown in Fig. 3. The terms a_x and g are the braking acceleration and gravitational acceleration as defined earlier.

To complete the analysis for the steady-state bicycle model, the braking forces on each axle are needed. Braking forces are often (and intentionally) distributed unequally between axles. Under severe braking, the front axle will have more normal force and will thus be able to generate more braking forces, and consequently in vehicles a brake proportioning valve activates above a certain brake command to shift additional brake inputs to the front tires (see Limpert, 1999). In this work, a simple braking model is used to split braking between each axle as the valve only activates at higher deceleration levels, generally higher than any seen in normal driving. To confirm this assumption, Table 1 shows the decelerations at which each vehicle's proportioning valve would initiate a reduction in rear tire braking force, for a zero-grade situation and for a 9% downgrade (9% downgrade is the steepest downgrade used in common practice on U.S. highways).

Four different decelerations are studied in this study: 0, −3, −11, and −15 ft/s^2 representing no braking, curve-entry braking, stopping-sight braking, and the minimum level of emergency braking, respectively. Using brake-proportioning valve settings for each representative vehicle as obtained from CarSim software documentation, the two highest decelerations in this study (−11 and −15 ft/s^2) may cause brake-proportioning valve activation.

In general the stopping sight distance (−11 ft/s^2) and emergency braking (−15 ft/s^2) decelerations would not be considered "steady-state" driving situations, as the vehicles' speed is changing too abruptly to satisfy the model assumptions. However, the equations in this analysis are "steady" in that they assume constant terms in the equations, including decelerations, and thus they will give estimates of necessary tire forces at the onset of the maneuver before speed changes significantly, precisely when skidding will most likely occur.

5. Transient Bicycle Model and Multi-Body Simulations

The transient bicycle model is identical in formulation to the steady-state model, except that the forces are summed to equal the inertia times acceleration rather than zero; details on this model can also be found in Pacejka (2006). The resulting differential equations are solved in this study using MATLAB/Simulink with a 0.0001 second time step and ODE45 variable time-step numerical solver. The primary benefit of the transient model versus the steady-state model is that it allows changing steering inputs, for example lane-change maneuvers.

Finally, a multi-body vehicle dynamics simulation is used to simulate vehicle outputs. For this study, CarSim and TruckSim software packages were used using default values for all vehicles. For both the transient bicycle model and the multi-body simulation models, the road profiles were imported in a manner that allowed the vehicle at least 10 s of straight-line approach to the curve to ensure that transient behavior due to initial conditions is completely settled out prior to curve entry.

Table 1
Decelerations at which brake proportioning valve activates.

Vehicle class	$a_{x,p}$, 0% grade	$a_{x,p}$, −9% grade
E-class sedan	−17.21 ft/s^2	−14.31 ft/s^2
E-class SUV	−12.82 ft/s^2	−9.92 ft/s^2
Full-size SUV	−10.92 ft/s^2	−8.02 ft/s^2

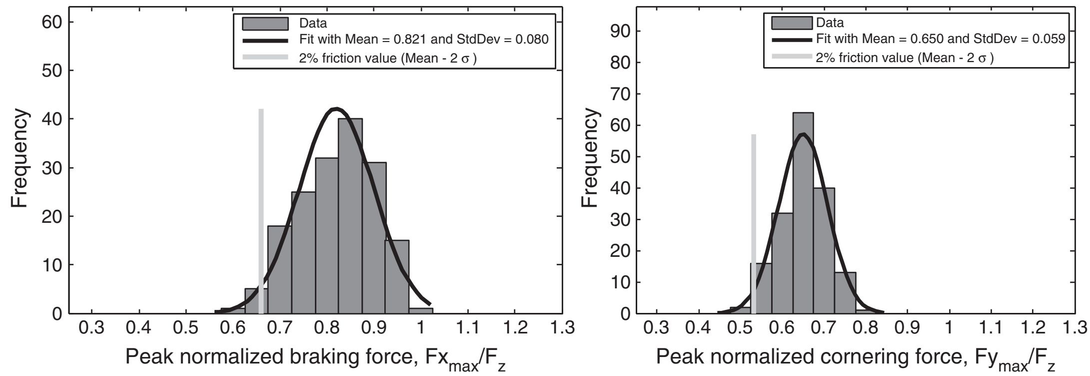

Fig. 4. Distribution of maximum friction for longitudinal (braking) and lateral (cornering) directions across all sites for passenger vehicle tires (85 mph).

5.1. Simulation Parameters and Friction Measurements

Vehicle simulation parameters were obtained by standard vehicle parameter sets used in CarSim and TruckSim for an E-class sedan, E-class SUV, compact sedan, full-sized SUV, single-unit truck, and a tractor semi-trailer vehicle under empty, half-loaded, and fully-loaded configurations. These values were compared to NHTSA-published datasets and peer-reviewed literature and found to quite close. Due to the limited scope of this paper, only the E-class sedan and SUV results can be discussed.

Lane-change durations were determined by experimentally measuring approximately 1,127 lane change events observed in video logs of the downgrade sites in this study. The results indicate that passenger vehicles took 3 s for a lane change (2.90 s with 0.82 std dev). Differences between left-to-right and right-to-left lane change durations were not found to be statistically significant. To represent lane changes in simulation, a duration of 3 s was used for the period of the single sine wave steering input. The amplitude of the sine wave was calculated for each vehicle to exactly produce a 12 foot amplitude lane change within the curve.

To obtain realistic friction supply estimates, friction values were obtained from comprehensive measurements at 5 different sites in the Eastern U.S., with 63 measurements at each site. The measured data were processed to populate coefficients in a LuGre tire model that predicts tire forces and friction ellipses in both the longitudinal (braking) and lateral (cornering) tire directions (de Wit, Olsson, Astrom, & Lischinsky, 1995). The principal axes of the ellipse – representing the maximum friction predicted by the tire curve – are used to predict maximum available friction values for wet roads at the 315 measurement locations, for both braking and cornering. Because the peak tire forces change with speed, this process was repeated for the different speed levels considered in this study (25 to 85 mph in 5 mph increments). This resulted in 2,184 different brake- and cornering-force friction curves.

The histograms of these tire–pavement curves were used to calculate the mean and minimum levels of friction supply for pure braking and pure cornering, at each measurement site and at each speed. The resulting friction values are normally distributed with a well-defined mean and standard deviation, allowing statistical definitions of friction supply for simulations. Specifically, the data from all road measurements were used to generate a histogram of friction values for each speed; an example of this is shown in Fig. 4. To incorporate a conservative approach into the design criterion, the lowest level of maximum friction supply considered in the analysis was assumed to be two standard deviations below the mean (e.g., a 2% friction value).

These mean and two-standard deviation "low" friction supply curves versus speed were then compared to the AASHTO maximum side friction curves used in horizontal curve design for both passenger car tires and trucks (Fig. 5). This figure shows that the friction supply curves for both the lateral (cornering) and longitudinal (braking) directions for both passenger vehicles and trucks are higher than the maximum friction demand curves (f_{max}) given by the AASHTO policy. Thus, current horizontal curve design policy appears to provide reasonable friction margins against skidding when the vehicle is only cornering or only braking. Consequently, if there is going to be an area of concern based upon AASHTO's current design policy, it will likely arise from the interaction of braking and cornering forces.

In contrast to the wet-road supply friction, the demanded friction levels are obtained from vehicle simulations that are run hereafter under "dry-road" assumptions. This choice accommodates friction transitions that commonly occur on roads but are hard to consider analytically. For example, a vehicle that is maneuvering on a dry road may encounter a wet patch of road within that maneuver. In such a case, the tires could be demanding forces on entrance to the maneuver that are from a dry road, but friction supply along subsequent wet portions of the road may be limited by wet-road conditions.

6. Results and Discussion

Fig. 6 shows a comparison of friction margins predicted by the point-mass model, steady-state bicycle model, and transient model for an E-class sedan maintaining a lane within a minimum-radius turn with no lane changes or braking. Two situations of superelevation are shown representing extremes: one at 4% and for 16%. The effect of superelevation is negligible except for speeds above 50 mph, at which speeds the friction margins on approach to the curve, not within the curve, become limiting at high speeds. In other words, the approach transition from level road to severely superelevated road gives worse friction margins than within the curve. This small sensitivity to

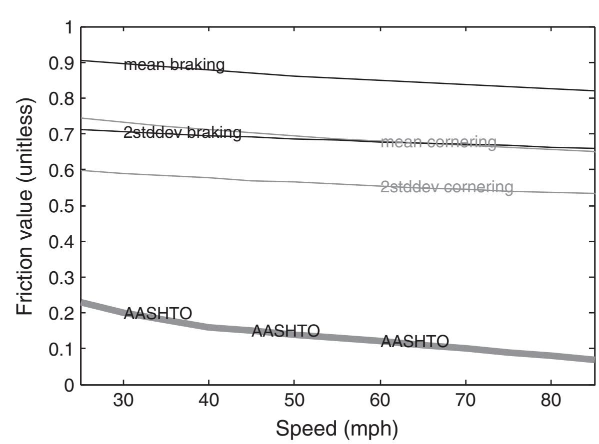

Fig. 5. Passenger vehicle maximum tire measurements of wet-tire friction in longitudinal (braking) and lateral (cornering) directions.

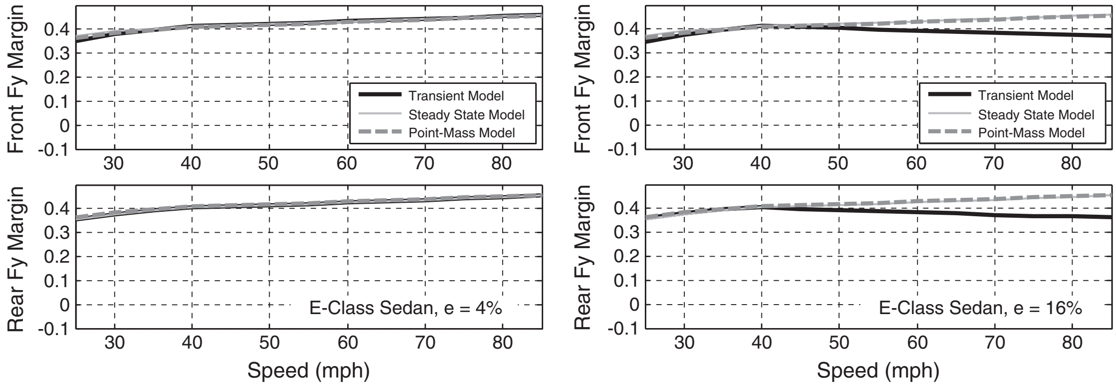

Fig. 6. Lateral friction margins from point-mass, steady state bicycle, and transient bicycle models for E-class sedan ($G = -9\%$, $e = 4$ and 16%) ($a_x = 0$ ft/s^2).

superelevation is an effect of the AASHTO design policy, which designs roadway curvature to precisely cancel the effects of superelevation. The differences between the various models for this situation is otherwise negligible, and thus the point-mass model, being simplest, is most appropriate for design in this brake-free, lane-change free situation.

Fig. 7 shows comparison of friction margins predicted by the point-mass model, steady-state bicycle model, and transient model for an E-class sedan performing a lane change in a minimum-radius curve, with no braking. One observes that the transient model predicts significantly lower friction margins on both the front and rear axles than does the steady-state model or the point-mass models, neither of which includes lane-change effects. What is surprising about the result is that the modest lane-change utilizes a significant fraction (roughly 75%) of the reserve friction margin. Nearly identical results were seen for truck lane changes, even though these drivers used a different lane-change duration. Thus, it appears that drivers performing lane-change maneuvers may be selecting the duration of the lane change (and hence aggressiveness of tire force usage) to utilize similar proportions of the reserve friction margin.

Shown in Fig. 8 is a comparison of friction margins predicted by the steady-state bicycle model versus the transient bicycle model for steady

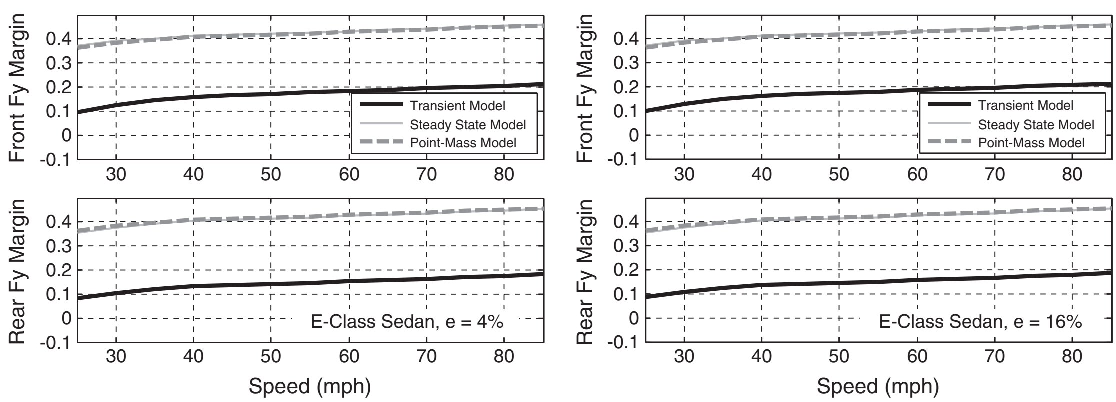

Fig. 7. Lateral friction margins from point-mass, steady-state bicycle, and transient bicycle models for E-class sedan ($G = -9\%$, $e = 4$ to 16%) ($a_x = 0$ ft/s^2 and lane change).

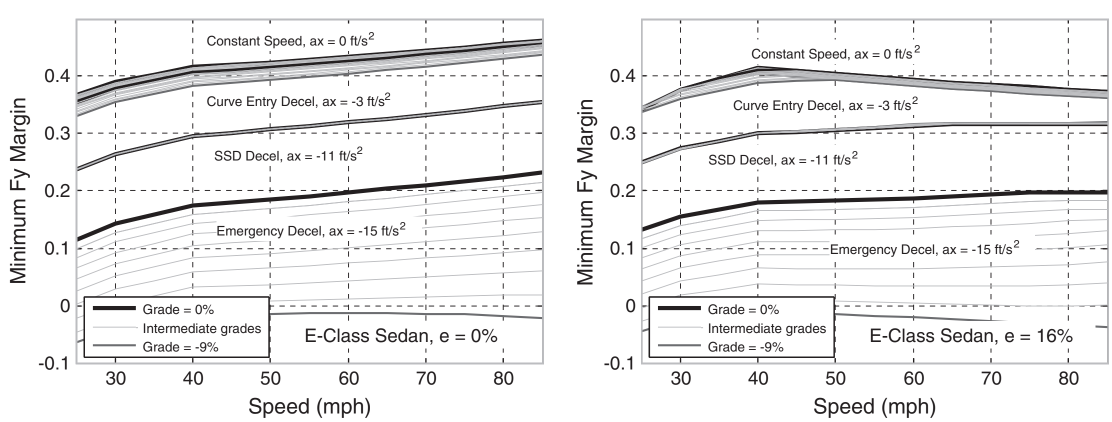

Fig. 8. Lateral friction margins from steady-state bicycle (left) and transient bicycle (right) models for E-class sedan ($G = 0$ to -9%, $e = 0$ and 16%) ($a_x = 0, -3, -11,$ and -15 ft/s^2).

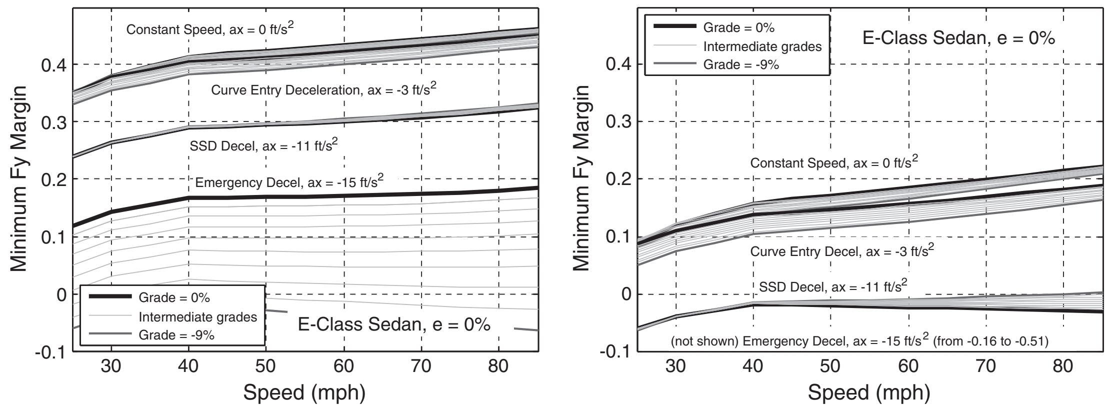

Fig. 9. Lateral friction margins while maintaining the same lane (left) and with a lane change for E-class sedan ($G = 0$ to -9%, $e = 0\%$) ($a_x = 0, -3, -11,$ and -15 ft/s^2).

lane-keeping but under different braking maneuvers, for an E-class sedan. The results are quite similar for both models, except above 50 mph for constant speeds and light braking. Again, these differences are due to the effects of the transition into the curve, rather than the curve itself.

Shown in Fig. 9 are plots comparing friction margins predicted by the steady-state bicycle model versus the transient bicycle model for lane changes under different braking maneuvers, for an E-class sedan. The results are quite dissimilar. Again, the lane-changes utilize a significant fraction of the friction margin. For stopping-sight decelerations (-11 ft/s^2) and emergency decelerations (-15 ft/s^2), negative friction margins are observed in the transient bicycle model that indicate a possibility of vehicle skidding in these situations. Note that the steady-state bicycle model does not capture these predictions.

Shown in Fig. 10 is a comparison of friction margins predicted by the transient bicycle versus the multi-body model. The results for the front axle are quite similar for both models, but for the rear tires the transient bicycle model predicts lower margins. Close analysis of the two model outputs showed that this difference is due to the dynamics of the tire and brake system that are neglected in the bicycle model, that cause the rear tire forces to not be as aggressive in the multi-body model for this situation. However, for slightly different timing of brake and steering, the multi-body model gives results quite similar to the transient model, thus showing that the multi-body model is very sensitive to parametric choices in the simulation with little appreciable benefit in understanding. Because their results are quite similar and the transient model is simpler, the transient bicycle model is more suited for roadway friction margin analysis.

7. Conclusions

The results of these simulations illustrate that for situations without lane changes, the point-mass model used by AASHTO is appropriate for friction margin analysis as long as one includes the friction ellipse to combine steering and braking effects. In situations with lane changes and severe braking, the most appropriate method to predict road friction margin appears to be the transient bicycle model. The multi-body vehicle simulation appears to be unnecessary for predicting friction margins and hence skidding events, except for very brief transient effects such as fast oscillations due to tire or brake dynamics. However, the results also indicate that there are specific maneuvers, namely braking events within lane changes and curves, which consistently predict the worst-case skidding events across all models. These results suggest that any vehicle model used for roadway safety analysis should include the effects of combined cornering and braking.

Acknowledgments

The authors gratefully acknowledge the support of the National Academy of Science Transportation Research Board, Project 15-39, in supporting portions of this study.

References

American Association of State Highway and Transportation Officials (2011). *A policy on geometric design of highways and streets.* Washington, DC: Author.

Chemistruck, H. M., Detweiler, Z. R., Ferris, J. B., Reid, A., & Gorsich, D. (2009). Review of current developments in terrain characterization and modeling, modeling and

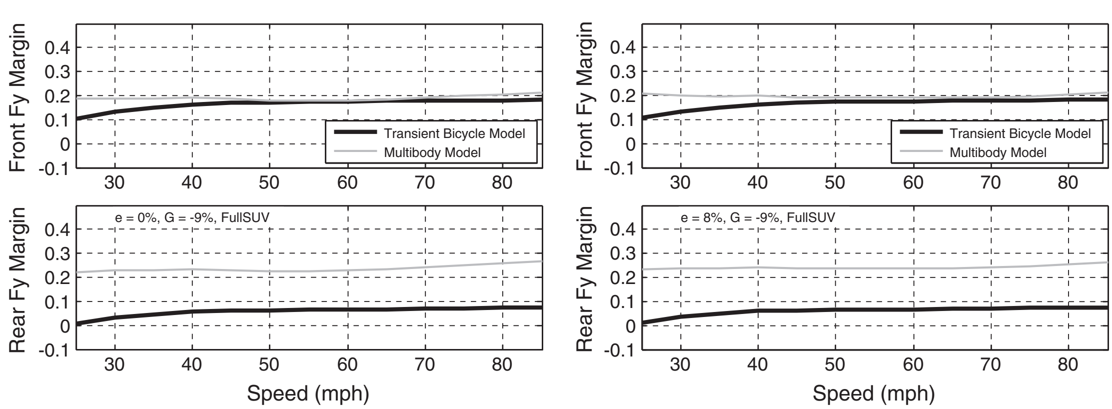

Fig. 10. Lateral friction margins from transient bicycle and multi-body models for full-size SUV ($G = -9\%$, $e = 0$ and 8%) ($a_x = -3$ ft/s^2 and lane change).

simulation for military operations IV. In Dawn A. Trevisani (Ed.), *Proc. of SPIE, Vol. 7348,73480N*.

de Wit, C., Olsson, H., Astrom, K. J., & Lischinsky, P. (1995). A new model for control of systems with friction. *IEEE Transactions on Automatic Control*, *40*(3).

Dembski, N., Rizzoni, G., Soliman, A., & Malmedahl, G. (2006, January). The development of a terrain severity measurement system. *In ASME 2006 international mechanical engineering congress and exposition*, (pp. 217–226). American Society of Mechanical Engineers.

Detweiler, Z. R., & John, B. F. (2010). Interpolation methods for high-fidelity three-dimensional terrain surfaces. *Journal of Terramechanics*, *47*(4), 209–217.

Kern, J., & Ferris, J. (2007). Development of a 3-D vehicle-terrain measurement system part I: Equipment setup. *Proceedings of the Joint North America Asia-Pacific ISTVS Conference and Annual Meeting of Japanese Society for Terramechanics, Fairbanks, AK*.

Limpert, R. R. (1999). *Brake design and safety*. *(SAE)*.

Pacejka, H. B. (2006). *Tire and vehicle dynamics*. : Society of Automotive Engineers, Inc.

Stine, J. S., Hamblin, B., Brennan, S. N., & Donnell, E. (2010, November). Analyzing the influence of median cross-section design on highway safety using vehicle dynamics simulations. *Accident Analysis and Prevention*, *42*(6), 1769–1777.

Varunjikar, T. (2011). *Design of horizontal curves with downgrades using low-order vehicle dynamics models*. University Park, PA: The Pennsylvania State University, Mechanical Engineering.

Alexander A. Brown received the BS, MS, and PhD degrees in mechanical engineering from Penn State University in 2008, 2012, and 2013 respectively. He is currently a post-doctoral scholar at Penn State University's Larson Transportation Institute. His research interests include passenger vehicle dynamics and vehicle automation with a focus on vehicle state and environment perception fusing mapped information with traditional sensors.

Sean N. Brennan received the BS degrees in mechanical engineering and physics from New Mexico State University in 1997 and the MS and PhD degrees in mechanical engineering from The University of Illinois at Urbana-Champaign in August 1999 and December 2002, respectively. He is an associate professor of mechanical engineering at the main campus of The Pennsylvania State University in University Park. His research interests include map-based dynamics and control of ground vehicles, mechatronics, and dimensional analysis.